

Performance analysis of inductive power transfer using JMAG-designer

Ismail Ahmat Mahadi, Jabbar Al-Fattah Yahaya

Department of Electrical Engineering, Faculty of Electrical and Electronics Engineers, Universiti Tun Hussein Onn Malaysia, Parit Raja, Malaysia

Article Info

Article history:

Received Dec 20, 2021

Revised Jul 18, 2022

Accepted Oct 6, 2022

Keywords:

Compensation topology

Inductive power transfer

JMAG-designer

Transfer efficiency

Wireless power transfer

ABSTRACT

Due to its advantage of sending electrical power from the transmitter source to the receiver load with no physical contact, wireless power transfer (WPT) has rapidly gained popularity in recent years. They can be used in a variety of applications, including induction cooking, mobile phone charging, radio frequency identification (RFID), and electric vehicles (EVs). Using JMAG-designer, a simulation of series-parallel inductive power transmission has been investigated in this research. This study aims to determine how the output power and efficiency change depending on how many coils turn in the transmitter and receiver. The number of coils turn in the transmitter is fixed which is 20 turns, the number of coils turn in the receiver is variable and ranges between 15 and 30, and the air gap or distance between the coupling coils is set at 10 cm. The selected frequency to be used in this simulation is between 10 and 50 kHz. According to the absorption result, the output power and efficiency rise when the receiver has more coil turns than the transmitter, and the output power and current rise along with an increase in resonance frequency.

This is an open access article under the [CC BY-SA](https://creativecommons.org/licenses/by-sa/4.0/) license.



Corresponding Author:

Ismail Ahmat Mahadi

Department of Electrical Power Engineering, Faculty of Electrical and Electronics Engineering

Universiti Tun Hussein Onn Malaysia

Persiaran Tun Dr. Ismail, 86400 Parit Raja, Johor, Malaysia

Email: ahtism900@gmail.com, ismailaht@ieee.org

1. INTRODUCTION

Normally, electric appliances such as mobile phones are powered by a cable that transports electricity from the power source to the load which is the device. However, they are inconvenient since they cannot be moved while charging, have broken cables, have the need to make an electrical connection during rainy weather, and pose safety issues [1], [2]. Although some electric equipment relies on a battery for movement, the batteries have various drawbacks, which make them uncomfortable such as size, capacity, weight, and efficiency [3]. Wireless power transfer (WPT) has been studied in the past decades to overcome this limitation. The advantage of WPT is that no mechanical contact is made while power is transferred from the transmitter windings to the receiver windings. Many applications use WPT such as biomedical equipment, electric vehicles (EVs), radio frequency identification (RFID), and medical implants [4]–[6].

The WPT technique is being quickly embraced in the transportation industry and several distinct field approaches are being employed for its implementation with varied changes of certain characteristics [7]. To achieve the highest power transfer efficiency, for instance, compensation topologies, frequency control, and inverter design are used, to achieve maximum transfer efficiency [8]. In WPT, a variety of techniques are used; nevertheless, they all primarily depend on the distance between the transmitter and receiver, the operating frequency, and how much power is being transferred [9]. Far-field fields and near-field fields are

two different types of fields used in WPT [10]. The contrast between the two varieties of fields is seen in Table 1.

Table 1. Comparison between far-field and near field

WPT	Far field	Near field
Range	Long	Short-Mid
Phenomenon	Coupled mode theory	Induction theory
Frequency	Megahertz	Kilo Hertz
Efficiency	Low	High

The advantage of WPT over traditional wiring is that it uses air to send energy from the desired source to the intended load. WPT uses both methods far-field and near-field to transmit power wirelessly. The far-field approach transmits energy from the source to the load using microwave, optical, and acoustic waves. Whereas the near-field majority of WPT approaches employed near-field electromagnetic induction, which consists of two different techniques: magnetic field induction, otherwise known as inductive power transfer (IPT), and electric field induction, otherwise known as capacitive power transfer (CPT) [11]–[13].

In WPT, electromagnetic radiation, electric coupling, and magnetic coupling are the three basic categories based on the principal operation. Microwaves can be used in electromagnetic radiation mode to complete a long-distance energy transfer. But, due to radioactive energy's omnidirectional nature in the far-field, this strategy is ineffectual and may even be dangerous. The other two techniques, on the other hand, do not emit radiation and can transfer near-field distance. The first one is CPT, it operates with two metal sheets for the transmitter and receiver as electrodes to transfer an electric field between them, but this technique is less common compared to the magnetic coupling method because the electric field is slightly more dangerous to the living organism compared to the magnetic field. The second method is magnetic coupling mode, which employs a magnetic field and is further subdivided into coupled magnetic resonance system (CMRS) and IPT [14]. IPT and CMRS utilize mutual induction, they have extremely straightforward concepts exactly like electrical transformers [6].

An IPT system uses an electromagnetic field (EMF) to transfer from the primary to the secondary through the air, so there is a large leakage EMF which leads to high reactive power and low transfer efficiency. To reduce that leakage a compensation circuit is used in the primary and secondary circuits which consist of capacitor banks connected either in series or parallel to the primary and secondary circuits of the system which are used as a compensation circuit. There are four types of capacitor bank connections also known as basic compensation topology, which are series-series (SS), series-parallel (SP), parallel-series (PS), and parallel-parallel (PP) [15]–[18].

Several factors contribute to the design of WPT, including the air gap between the coupling coils, the number and position of coils turn in the transmitter and receiver's pad, the frequency of the system, and the compensation capacitors. All these factors lead to either increase or decrease in the efficiency of the WPT system. According to [19]–[22], all have used the primary coils turn is more than the secondary, and the system obtained a high efficiency. However, based on [8], [23]–[25], they used the same number of primary and secondary coil turn, but they obtained slightly lower efficiency as compared to the previous condition. All these factors contribute to the design of WPT. The purpose of this study is to examine the impact of changing the secondary coil's number of turns when the primary coil's number of turns is fixed. Additionally, the efficiency and output power at various frequencies are between 10 and 50 kHz. SP compensation topology is the one used in this system.

2. BASIC CONCEPT OF WIRELESS POWER TRANSFER MODULE

WPT is made up of the transmitter and receiver coils, N_p and N_s respectively. The number of turns on the transmitter and receiver coils rely on the output voltage, to get a greater output value, N_s must have more turns than N_p . The transmitter coil is linked to the power supply, while the receiver coil is linked to the battery or load. The voltage differential between the coupling coils is produced in a manner similar to that of a transformer by varying the number of coil turns in the transmitter pad compared with the number of coils turns in the receiver pad [26]. Figure 1 displays the fundamental representation of the WPT system. It is made up of a high-frequency inverter, a primary and secondary coil, compensation capacitors, and a converter that charges the battery.

The high-frequency AC output of the inverter is fed into the compensation capacitor, which is used to improve the circuit's performance. Power is transferred between the coupling coils, which are separated by an air gap. The battery pack, which is located on the secondary side of the circuit, receives the rectifier DC output and charges it [27], [28].

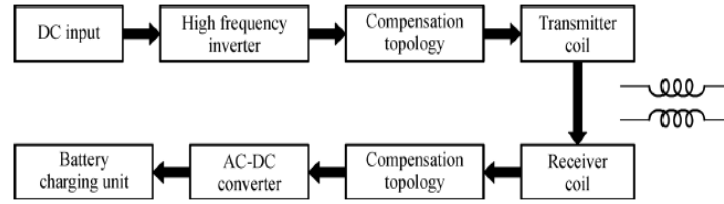


Figure 1. Basic block diagram of WPT

3. METHOD

The transmitter circuit, receiver circuit, and coupling devices are the three basic components of WPT, as represented in Figure 2. The power source is directly connected to the transmitter, where it is transformed into an EMF and transmitted via the coupling device. Contrarily, the receiver uses its coupling mechanism to capture the radiated energy and transform it back into DC or AC so that the load can use it. Each technique has its specifications, such as power converter circuits, operating frequencies, and coupling coils which are transmitter and receiver, which affect the transfer distance capability and efficiency of the system, the block diagram in Figure 2 illustrates the fundamental and common principle of WPT [29].

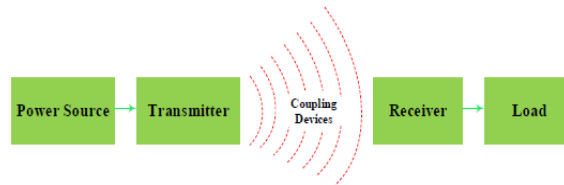


Figure 2. The basic concept of WPT system

Figure 3 illustrates the circuit diagram used in this simulation which consists of the source, primary and secondary coil and capacitor, and resistive lead. To design WPT in JMAG-designer, first, the design must be drafted in the geometry editor. It is used to sketch the transmitter and receiver core and the coil of the system. After the sketch is finalized in the geometry editor, then the sketch is imported to the main software which is the JMAG-designer, where all the circuit components, frequency, and the condition of the system are simulated. The coupling coefficient and the mutual inductance of the coil can be expressed as [30].

$$M = k\sqrt{L_p L_s} \tag{1}$$

The efficiency of power transfer for both calculated and simulated can be obtained using as follows:

$$\eta = \frac{P_L}{P_{in}} \times 100\% \tag{2}$$

$$\eta = \frac{P_L}{P_{in}} = \frac{R_L I_s^2}{R_p I_p^2 + (R_s + R_L) I_s^2} \tag{3}$$

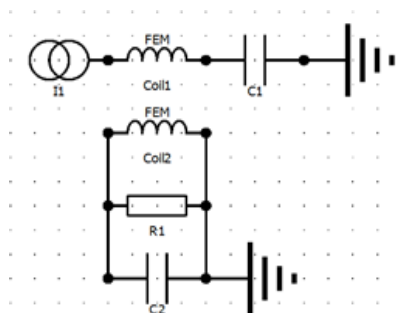


Figure 3. The proposed circuit of the simulation

4. RESULTS AND DISCUSSION

Table 2 compares the previous studies to this work, which reveals that [22], uses a higher number of turns in the coupling coils, but their frequency is low, therefore the efficiency obtain is low. Utilized [8] more coil turns and a higher frequency, but because of the distance between the coupling coil, the efficiency obtained is likewise low. Furthermore, the efficiency in [21], [25] is almost similar, the first applied a higher frequency value and smaller air gap between the coupling coil, while the second used a lower frequency value and a larger number of coil turns and air gap between the coupling coil. Lastly, the frequency and airgap used in [21] and this design are both the same, but this design has less coil turn in its coupling coil than that in the prior study, but this design has better efficiency than [21].

Table 2. Comparison between previous design and this design

Journal	Number of coils turns	Air gap (cm)	Efficiency (%)	Frequency (kHz)	Output power
[22]	N1=70, N2=100	10	86	10	100 w
[8]	N1=39, N2=50	4	72.7	100	18.5 w
[25]	N1=25, N2=25	1	82.6	150	N/A
[21]	N1=50, N2=20	100	85	50	N/A
[24]	N1=2, N2=2	15	88.05	85.5	2.86 kw
[20]	N1=31, N2=4	20	90	182	500 w
This design	N1=20, N2=30	100	94	50	148.13 w

The results of the simulation discussed below were obtained using the finite-element method (FEM) JMAG-designer, and the system design parameters and components used in the simulation are provided in Tables 3 and 4. The FEM 3D system design is presented in Figure 4. Figure 5 illustrates the magnetic flux between the transmitter and receiver. The air gap between the coupling coil is set to be 100 mm. The graphs presented in Figure 6 demonstrate that the number of turns on the coil influences system performance.

Table 3. The system parameters and specification

Parameter	Specification
Number of coils turns in the primary	20
Number of coils turns in secondary	15-30
Inner diameter of the coil	80 mm
Outer diameter of the coil	300 mm
Conductor radius	5 mm
Coil material	Copper
Coil shape	Circular
Core diameter	320 mm
Core radius	5 mm
Core material	Ferrite
Airgap	50-300 mm

Table 4. The parameters and the value used in the simulation

Parameter	Symbol	Value
Input current source	I_P	15 A
Resonant frequency	F_S	10-50 kHz
Mutual inductance	M	3-65 μ H
Transmitter capacitance	C_T	2.95 nF
Receiver capacitance	C_R	2.95 nF
Transmitter constant resistor	R_T	83.65 m Ω
Receiver constant resistor	R_R	83.65 m Ω
Resistive load	R_L	100 Ω



Figure 4. The 3D FEM system design

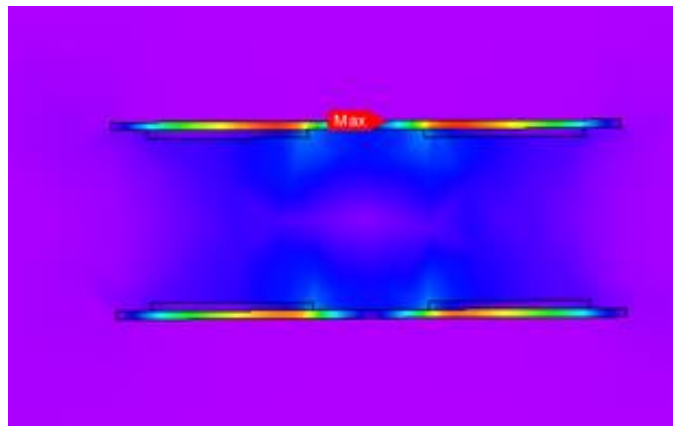


Figure 5. The magnetic flux of the coil

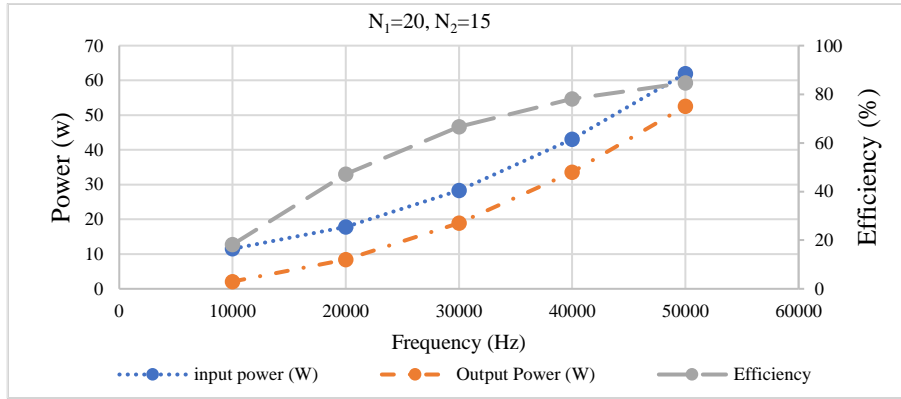
Tables 5 and 6 present the simulation result of the efficiency and manual calculation results where the formula is taken from (2) for 50 kHz operating frequency and 15 an input current. When the primary coil has, fewer coil turns compared to the secondary coil, the efficiency in the manual calculation result is better than the simulation result, as shown in Table 6, whereas when the receiver coil has more turns than the transmitter coil, the result of the simulation has better efficiency compared to the manual calculation. Figure 6(a) the output power is around 51 w when the primary side has 20 turns and the secondary has 15, and the efficiency is about 83% at 50 kHz operating frequency and 18% at 10 kHz frequency. When the secondary coil's turns increase as indicated in Figure 6(b). At the resonance frequency of 50 kHz, both the output power and efficiency increase to 88 w and 90.8%, respectively. When the secondary coil's number of turns is raised, the output power also rises and the efficiency improves, as shown in Figures 6(c) and (d), the outcome is the same as the prior one.

Table 5. Simulation result

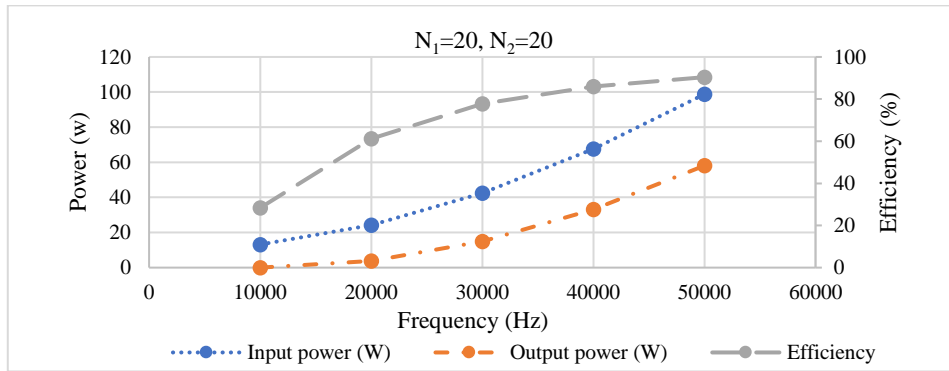
Output power (w)	Number of turns in secondary coil	Efficiency (%)	Frequency (kHz)
51.8	15	83	50
88.1	20	90.8	50
123.65	25	92.8	50
148.13	30	94	50

Table 6. Manual calculation result

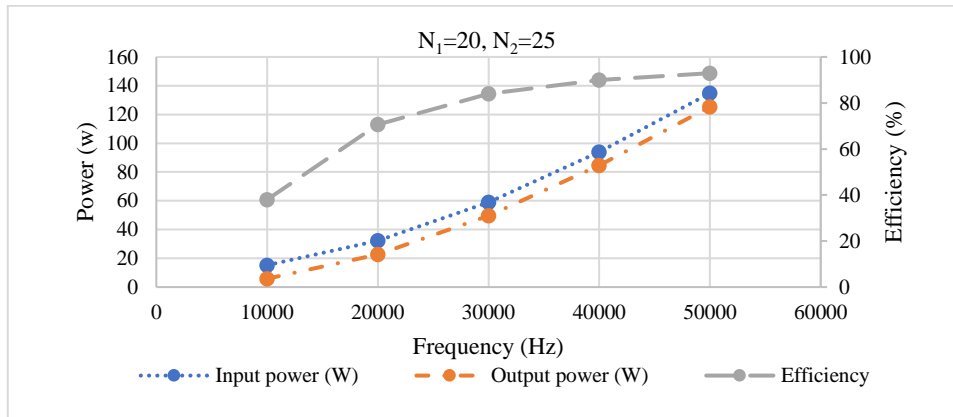
Output current (A)	Number of turns in secondary coil	Efficiency (%)	Frequency (kHz)
1.02	15	84	50
1.3	20	90	50
1.45	25	91.7	50
1.5	30	92.2	50



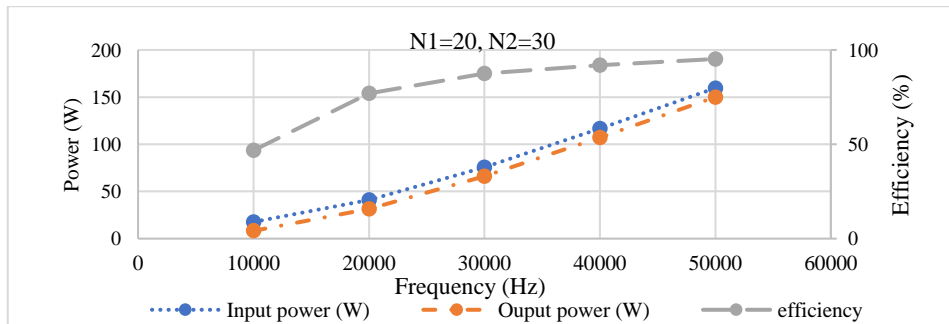
(a)



(b)



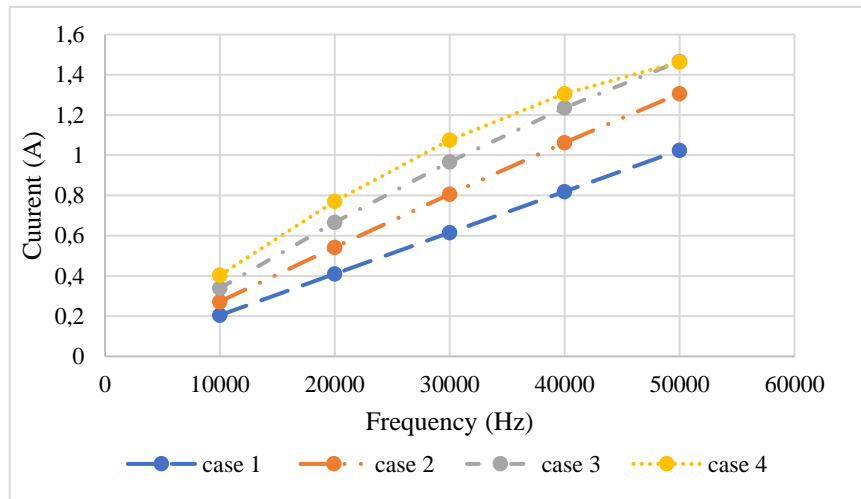
(c)



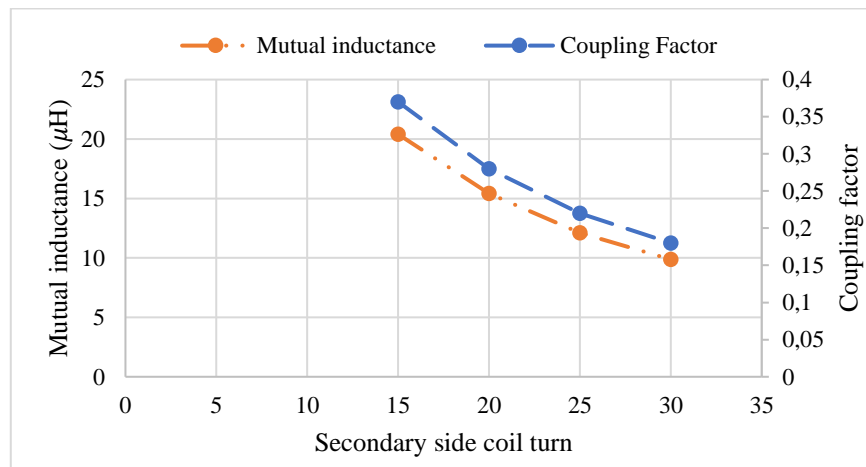
(d)

Figure 6. The frequency vs power and efficiency (a) $N_1=20, N_2=15$, (b) $N_1=20, N_2=20$, (c) $N_1=20, N_2=25$, and (d) $N_1=20, N_2=30$

Similar to how the power increases with frequency and secondary coil turn, the current similarly rises. Figure 7(a) illustrates this. When $N_1 > N_2$, in case 1 the current value is close to 1A, at 50 kHz. Whereas, in case 2, when $N_1 = N_2$ the current slightly increases. Furthermore, in cases 3 and 4, when $N_1 < N_2$ the current value is the highest compared to the previous two cases. Therefore, it can be stated that the system performs better in terms of output power and efficiency when the receiver coil has more turns than the transmitter coil. regarding Figure 7(b). It displays a graph between the receiver's side number of turns, the mutual inductance, and the coefficient of the coupling coil. Because the coupling coefficient as shown in (1), and Table 7, when the number of coils turning on the secondary, or receiver side, is more than on the transmitter side the mutual inductance and coefficient of coupling values drop.



(a)



(b)

Figure 7. Shows the (a) frequency vs current value and (b) secondary coil turn vs coupling coefficient k and mutual inductance M

Table 7. Comparison of M and k when coil at N_2 increases

Number of secondary coil turn	Coupling coefficient k	Mutual inductance M (μH)
15	0.37	20
20	0.27	14.8
25	0.22	12

5. CONCLUSION

In conclusion, this study uses JMAG-designer to analyze the system design parameters such as efficiency, frequency, and secondary coil number of turns. The analysis demonstrates that frequency and

efficiency are directly correlated, meaning that as the frequency rises, the system's power would rise along with it. Additionally, when the operating frequency is fixed and the number of coils turns on the receiver side more than the primary side, then the value of the output power and efficiency increase.

ACKNOWLEDGEMENTS

The author would like to acknowledge that this work is supported by the Ministry of Higher Education (MOHE) through Fundamental Research Grant Scheme (FRGS) (FRGS/1/2019/TK04/UTHM/03/14) and Universiti Tun Hussein Onn Malaysia (UTHM).




REFERENCES

- [1] M. Yilmaz and P. T. Krein, "Review of battery charger topologies, charging power levels, and infrastructure for plug-in electric and hybrid vehicles," *IEEE Transactions on Power Electronics*, vol. 28, no. 5, pp. 2151–2169, 2013, doi: 10.1109/TPEL.2012.2212917.
- [2] S. Al-Chlaihawi, A. H. Tawafan, and F. K. Abd, "Experimental installation of wireless power transfer system based on the series resonance technology," *International Journal of Power Electronics and Drive Systems (IJPEDS)*, vol. 11, no. 4, pp. 1693–1700, Dec. 2020, doi: 10.11591/ijpeds.v11.i4.pp1693-1700.
- [3] P. Machura and Q. Li, "A critical review on wireless charging for electric vehicles," *Renewable and Sustainable Energy Reviews*, vol. 104, pp. 209–234, Apr. 2019, doi: 10.1016/j.rser.2019.01.027.
- [4] J. Shin, S. Shin, Y. Kim, S. Lee, B. Song, and G. Jung, "Optimal current control of a wireless power transfer system for high power efficiency," in *2012 Electrical Systems for Aircraft, Railway and Ship Propulsion*, Oct. 2012, pp. 1–4. doi: 10.1109/ESARS.2012.6387426.
- [5] N. X. Yin, S. Saat, S. H. Husin, Y. Yusop, and M. R. Awal, "The design of IPT system for multiple kitchen appliances using class E LCCL circuit," *International Journal of Electrical and Computer Engineering (IJECE)*, vol. 10, no. 4, pp. 3483–3491, Aug. 2020, doi: 10.11591/ijece.v10i4.pp3483-3491.
- [6] I. Alhamrouni, M. Iskandar, M. Salem, L. J. Awal, A. Jusoh, and T. Sutikno, "Application of inductive coupling for wireless power transfer," *International Journal of Power Electronics and Drive Systems (IJPEDS)*, vol. 11, no. 3, pp. 1109–1116, Sep. 2020, doi: 10.11591/ijpeds.v11.i3.pp1109-1116.
- [7] P. S. Subudhi and K. S, "Wireless power transfer topologies used for static and dynamic charging of EV battery: a review," *International Journal of Emerging Electric Power Systems*, vol. 21, no. 1, pp. 1–34, Feb. 2020, doi: 10.1515/ijeeps-2019-0151.
- [8] A. Elahi, A. A. Amin, U. T. Shami, M. T. Usman, and M. S. Iqbal, "Efficient wireless charging system for supercapacitor-based electric vehicle using inductive coupling power transfer technique," *Advances in Mechanical Engineering*, vol. 11, no. 11, pp. 1–10, Nov. 2019, doi: 10.1177/1687814019886960.
- [9] M. A. Hassan and A. Elzawawi, "Wireless power transfer through inductive coupling," *Recent Advances in Circuits*, pp. 115–118, 2015.
- [10] K. Y. Lum, J.-S. Chow, and K. H. Yiau, "Wireless power transfer framework for minirobot based on resonant inductive coupling and impedance matching," *International Journal of Power Electronics and Drive Systems (IJPEDS)*, vol. 11, no. 1, pp. 317–325, Mar. 2020, doi: 10.11591/ijpeds.v11.i1.pp317-325.
- [11] N. Hasan and T. Saha, "A single-phase bidirectional AC-AC converter with H-bridge energy buffer for wireless power transfer applications," *International Journal of Power Electronics and Drive Systems (IJPEDS)*, vol. 13, no. 1, pp. 191–199, Mar. 2022, doi: 10.11591/ijpeds.v13.i1.pp191-199.
- [12] Z. Zhang, H. Pang, A. Georgiadis, and C. Cecati, "Wireless power transfer—an overview," *IEEE Transactions on Industrial Electronics*, vol. 66, no. 2, pp. 1044–1058, Feb. 2019, doi: 10.1109/TIE.2018.2835378.
- [13] F. K. A. Rahman, S. Saat, Y. Yusop, S. H. Husin, and M. H. Jamaluddin, "Efficiency comparison of capacitive wireless power transfer for different materials," *International Journal of Power Electronics and Drive Systems (IJPEDS)*, vol. 11, no. 1, pp. 200–212, Mar. 2020, doi: 10.11591/ijpeds.v11.i1.pp200-212.
- [14] L. Sun, D. Ma, and H. Tang, "A review of recent trends in wireless power transfer technology and its applications in electric vehicle wireless charging," *Renewable and Sustainable Energy Reviews*, vol. 91, pp. 490–503, Aug. 2018, doi: 10.1016/j.rser.2018.04.016.
- [15] N. T. Diep, N. K. Trung, and T. T. Minh, "Wireless power transfer system design for electric vehicle dynamic charging application," *International Journal of Power Electronics and Drive Systems (IJPEDS)*, vol. 11, no. 3, pp. 1468–1480, Sep. 2020, doi: 10.11591/ijpeds.v11.i3.pp1468-1480.
- [16] M. A. A. Roslan, N. N. Nanda, and S. H. Yusoff, "Series-series and series-parallel compensation topologies for dynamic wireless charging," *IJUM Engineering Journal*, vol. 22, no. 2, pp. 199–209, Jul. 2021, doi: 10.31436/ijumej.v22i2.1660.
- [17] C. Jiang, K. T. Chau, C. Liu, and C. H. T. Lee, "An overview of resonant circuits for wireless power transfer," *Energies*, vol. 10, no. 7, p. 894, Jun. 2017, doi: 10.3390/en10070894.
- [18] X. Mou, D. T. Gladwin, R. Zhao, and H. Sun, "Survey on magnetic resonant coupling wireless power transfer technology for electric vehicle charging," *IET Power Electronics*, vol. 12, no. 12, pp. 3005–3020, Oct. 2019, doi: 10.1049/iet-pel.2019.0529.
- [19] M. Rehman, P. Nallagownden, and Z. Baharudin, "Efficiency investigation of SS and SP compensation topologies for wireless power transfer," *International Journal of Power Electronics and Drive Systems (IJPEDS)*, vol. 10, no. 4, pp. 2157–2164, Dec. 2019, doi: 10.11591/ijpeds.v10.i4.pp2157-2164.
- [20] Y.-C. Hsieh, Z. Lin, M. Chen, H. Hsieh, Y. Liu, and H.-J. Chiu, "High-efficiency wireless power transfer system for electric vehicle applications," *IEEE Transactions on Circuits and Systems II: Express Briefs*, vol. 64, no. 8, pp. 942–946, Aug. 2017, doi: 10.1109/TCSII.2016.2624272.
- [21] A. Purwadi, A. Rizaiawan, A. P. Pohan, D. C. Abdillah, and M. D. G. Wijaya, "Study and design high-frequency resonant inductive power transfer for application of wireless charging electric vehicles," in *2018 5th International Conference on Electric Vehicular Technology (ICEVT)*, Oct. 2018, pp. 179–187. doi: 10.1109/ICEVT.2018.8628380.
- [22] M. Elwalaty, M. Jemli, and H. B. Azza, "Modeling, analysis, and implementation of series-series compensated inductive coupled power transfer (ICPT) system for an electric vehicle," *Journal of Electrical and Computer Engineering*, pp. 1–10, Jan. 2020, doi: 10.1155/2020/9561523.




- [23] S. Kuzey, S. Balci, and N. Altin, "Design and analysis of a wireless power transfer system with alignment errors for electrical vehicle applications," *International Journal of Hydrogen Energy*, vol. 42, no. 28, pp. 17928–17939, Jul. 2017, doi: 10.1016/j.ijhydene.2017.03.160.
- [24] Z. Li, C. Zhu, J. Jiang, K. Song, and G. Wei, "A 3-kW wireless power transfer system for sightseeing car supercapacitor charge," *IEEE Transactions on Power Electronics*, vol. 32, no. 5, pp. 3301–3316, May 2017, doi: 10.1109/TPEL.2016.2584701.
- [25] M. Kavitha, P. B. Bobba, and D. Prasad, "Comprehensive mathematical modelling and experimental analysis of a wireless power transfer system for neighborhood electric vehicles," in *2015 IEEE International WIE Conference on Electrical and Computer Engineering (WIECON-ECE)*, Dec. 2015, pp. 275–279. doi: 10.1109/WIECON-ECE.2015.7443916.
- [26] F. Azhar, N. A. M. Nasir, A. L. Hakim, R. N. Firdaus, and C. V. Aravind, "Basic characteristics of wireless power transfer," *Journal of Engineering Science and Technology*, vol. 14, pp. 168–178, 2019.
- [27] P. S. R. Nayak and D. Kishan, "Performance analysis of series/parallel and dual side LCC compensation topologies of inductive power transfer for EV battery charging system," *Frontiers in Energy*, vol. 14, no. 1, pp. 166–179, 2020, doi: 10.1007/s11708-018-0549-z.
- [28] I. A. Mahadi and J. A.-F. Yahaya, "Performance analysis of different shielding material for a 100W wireless power transfer system," *Journal of Physics: Conference Series*, vol. 2319, no. 1, pp. 1–10, Aug. 2022, doi: 10.1088/1742-6596/2319/1/012006.
- [29] M. T. Nguyen *et al.*, "Electromagnetic field based WPT technologies for UAVs: A comprehensive survey," *Electronics*, vol. 9, no. 3, p. 461, Mar. 2020, doi: 10.3390/electronics9030461.
- [30] P. K. Joseph and D. Elangovan, "A review on renewable energy powered wireless power transmission techniques for light electric vehicle charging applications," *Journal of Energy Storage*, vol. 16, pp. 145–155, Apr. 2018, doi: 10.1016/j.est.2017.12.019.

BIOGRAPHIES OF AUTHORS



Ismail Ahmat Mahadi    is a postgraduate research student at Universiti Tun Hussein Onn Malaysia (UTHM), he received his bachelor's degree in Electrical Engineering from the same university in 2020. Currently, he is pursuing his master's degree in UTHM in Power Electronics focusing on wireless power transfer. His research interests include control strategies for AC high-frequency inverters and wireless power transfer. He can be contacted at email: ahtism900@gmail.com, or ismailaht@ieee.org.



Jabbar Al-Fattah Yahaya    is a senior lecturer at the Department of Electrical Engineering, Universiti Tun Hussein Onn Malaysia, Malaysia, where he has been a faculty member since 2017. Dr. Jabbar graduated with B.Eng. degree in Electronic Engineering from the University of Leeds, UK, in 2005, and an M.Eng. in Electrical Engineering from Universiti Malaya, Malaysia in 2010. He completed his Ph.D in Electrical Power Engineering from Universiti Tenaga Nasional, Malaysia, in 2017. His research interests are primarily in power electronics (electric power conversion, EV, renewable energy systems (RES), HVDC, control), power systems (arch flash analysis), and digital signal processing (DSP). He can be contacted at email: jabbar@uthm.edu.my.